Journal of Materials Chemistry B

Accepted Manuscript

ROYAL SOCIETY OF CHEMISTRY

www.rsc.org/materialsB

Journal Name

RSCPublishing

COMMUNICATION

Floating tablets from mesoporous silica nanoparticles

iCite this: DOI: 10.1039/x0xx00000x

Prasanna Lakshmi Abbaraju,[a] Anand kumar Meka,[a] Siddharth Jambhrunkar,[a] Jun Zhang,[a] Chun Xu,[a] Amirali Popat,*[b,c] and Chengzhong Yu*[a]

Received 00th January 2012,
Accepted 00th January 2012

DOI: 10.1039/x0xx00000x

www.rsc.org/

Novel floating tablets are designed using mesoporous silica nanoparticles for enhancing the drug delivery performance of both hydrophobic and hydrophilic drugs compared to conventional floating tablets.

Since the first report of ordered mesoporous materials in the early 1990s,[1] great attention has been paid to this family of materials due to their unique properties (e.g., easy synthesis, tunable structures, controllable surface chemistry)[2, 3] and a broad range of applications.[4-6] Recently, mesoporous silica nanoparticles (MSNs) have attracted enormous interest in drug delivery.[7] The large surface area and high pore volume of MSNs render a high efficiency to load cargo molecules, while the adjustable pores with a range of sizes can be used to control the drug release in a sustainable manner.[8, 9] MSNs have been demonstrated as targeted delivery systems to tumor cells[10, 11] and as stimuli-responsive systems[12-14]. MSNs have also been used in developing oral tablets because the oral route is still the preferable route of drug administration.[15, 16] However, there is no report on using MSNs in localised drug delivery for the upper region of gastrointestinal tract (GIT), i.e., stomach.

High residence time and local drug release in stomach is prerequisite for the drugs with narrow absorption window in upper GIT, and poor solubility or degradation in small intestine.[17] Various approaches have been developed for retaining a dosage form in stomach.[18, 19] Among these floating delivery system is considered as an effective technique.[20-22] A successful example of floating drug delivery systems is floating tablets.[23] Traditionally, floating phenomenon in floating tablets is achieved by using swellable polymers or polymer mixtures and gas generating agents.[17] However, for polymer based floating systems, controlling the release of highly water-soluble drug is limited.[24] Moreover, drug and polymer are generally physically mixed which does not aid in enhancing solubility of inherently insoluble drugs. In light of the advantages of MSNs in solubility enhancement[25] and controlled drug release,[26] it is hypothesised that a floating tablet based on MSNs will provide unprecedented benefits to address the limitations of conventional polymer based floating tablets.

In this communication, we report the first example of novel floating tablets based on MSNs for the localised drug release. As shown in Scheme 1A, MCM-41[1] type MSNs are chosen as drug carriers. Hydroxypropylmethylcellulose (HPMC) is chosen as a gelling agent due to its non-toxic nature, easy compression and swelling properties, which is widely used in oral and topical pharmaceutical formulations. Sodium bicarbonate is used as a gas generating agent. The floating tablet is prepared by blending drug loaded MSNs, HPMC and sodium bicarbonate (Scheme 1B) and compressing into tablet (Scheme 1C) using a single punch tablet compression machine. Curcumin and captopril are chosen as model hydrophobic and hydrophilic drugs respectively to demonstrate the application of novel MSNs based floating tablet. The resultant tablets showed extensive floating behaviour (>12 h) with improved dissolution rate and enhanced solubility for curcumin while extended release in case of captopril (Scheme 1D), providing a leap forward towards new application of mesoporous materials in localized oral drug delivery.

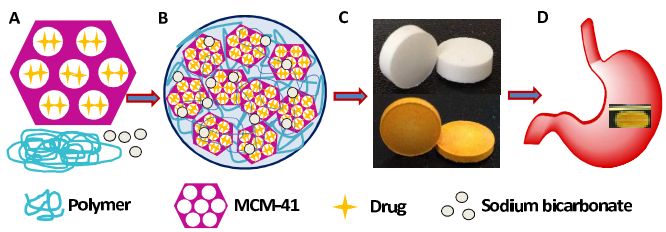

Scheme 1 Schematic representation of floating tablets made from drug loaded MCM-41, polymer and sodium bicarbonate (A). After blending and compression (B), captopril (white colored) and curcumin (yellow) floating tablets are obtained (C), which can float in stomach >12 h (D).

MCM-41 type MSNs were used in this study and prepared according to published methods[27] with slight variations (see ESI†). Calcined MCM-41 with two different pore sizes (2.1 and 1.7 nm) were used and the pore size adjustment was performed by a reported vacuum-assisted vapour deposition (VVD) process[25] (ESI†). The X-ray diffraction (XRD) patterns (Fig. S1A, ESI†) of calcined MCM-41 before and after VVD process both showed three well resolved peaks at 2θ of 2.68, 4.76 and 5.42°, which can be indexed as 100, 110, and 200 reflections of an ordered two dimensional hexagonal mesostructure. For MCM-41 after VVD process, the intensity of 110 and 200 peaks was decreased due to the decreased scattering contrast between the pore and silica walls.[28] This is evidenced from the N_2 adsorption-desorption analysis. Comparing the isotherms of calcined MCM-41 before and after VVD process (Fig. S1B, ESI†), the capillary condensation step shifted to a lower relative pressure range after VVD treatment, reflecting a pore size reduction from 2.1 to 1.7 nm (Fig. S1C, ESI†), in accordance with our previous results.[25] The surface areas and pore volumes are summarised in Table S1 (see ESI†).

Scanning electron microscopy (SEM) and transmission electron microscopy (TEM) were used to study the nanostructure of MCM-41. SEM images of two MCM-41 materials showed a spherical morphology with particle sizes of ~120 nm (Figs. S2c and d, ESI†). TEM images of both materials showed stripe-like or hexagonal pattern (Figs. S2a, b, ESI†), typical of MCM-41 materials.[29]

Because MSNs have not been used in the formulation of floating tablets, screening tests were conducted to optimise the floating tablet formulation by increasing the amount of MCM-41. The compositions of floating tablets (F0-FD) are shown in Table S2, ESI†. F0 is conventional polymer based, while FA-FD has a silica weight ratio of 42, 55, 58, and 62%, respectively. All tablets floated in simulated gastric fluid (SGF, pH 1.2) longer than 12 h. The silica content after 12 h of floating test decreased as the amount of silica increased (Fig. S3B, ESI†). FA with the initial silica ratio of 42% has the highest retention ratio of 80%. An initially larger MCM-41 content is beneficial for a higher dosage form, while the silica content remained in the tablet after floating is important to reduce the unwanted entry of drug into intestine. Consequently, the silica content of 42% was chosen as the optimised ratio (FA) in the following studies.

SEM was also used to investigate the morphology of floating tablets. A typical cross-section SEM images of FA is presented in Fig. 1a, showing a homogenous distribution of MCM-41 particles in the tablet. The HPMC (see SEM image in Fig. S2e, ESI†) and other ingredients cannot be seen in the tablet, suggesting a homogenous distribution of all ingredients.

After 12 h of floating test, the SEM image of F0 prepared without silica nanoparticles revealed a porous structure (Fig. S2f, ESI†). The pores are generated by entrapped CO_2 produced by the reaction of sodium bicarbonate with HCl in the gastric juice (pH 1.2). In contrast, the SEM image of FA prepared in the presence of MSNs after floating for > 12 h still showed homogeneously distributed MCM-41 nanoparticles in the polymer matrix (Fig. 1b), suggesting that HPMC play a dual role of gelling agent to entrap both gas and MSNs throughout the dissolution process.

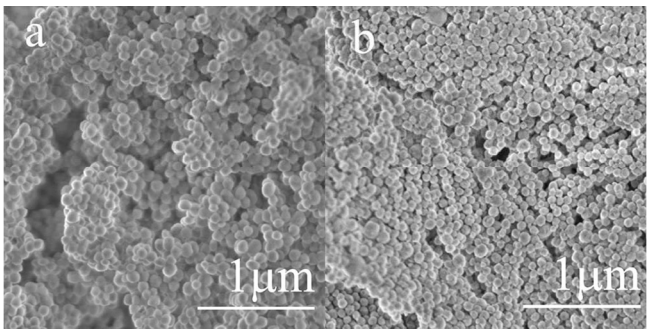

Fig. 1 Cross-sectional SEM images of (a) floating tablet with MSNs and (b) after 12 h of dissolution study.

In order to prepare a drug loaded floating tablet, curcumin (Cur) was separately loaded into two calcined MCM-41 with different pore sizes by a rotary evaporation method (see ESI†). Curcumin loaded MCM-41 samples were characterised by thermogravimetric analysis (TGA), differential scanning calorimetry (DSC), XRD and N_2 adsorption-desorption. TGA (Fig. S4, and Table S1, ESI†) showed that the weight percentage of curcumin was 20.0% and 20.9% in Cur-MCM-41(1.7nm) and Cur-MCM-41(2.1nm) respectively. Sharp diffraction peaks were observed in 2θ range of 5-40° for both pure curcumin and the physical mixture of curcumin and MCM-41 as observed from wide-angle XRD patterns (Fig. S5A, ESI†). Pure MCM-41 showed no diffraction peaks in 2θ range of 5-40°, indicating its amorphous nature. After loading curcumin into MCM-41, no obvious diffractions of curcumin were observed, suggesting that the drug has been successfully loaded as nano-aggregates into the pore channels of MCM-41 in an amorphous state. This conclusion is further confirmed by DSC analysis. The DSC curve (Fig. S5B, ESI†) of pure curcumin showed a sharp endothermic peak at 172 °C corresponding to its melting point. After loading curcumin into MCM-41 this peak showed very week intensity, suggesting that the crystallinity of curcumin has been significantly reduced after loading inside the pore channels.

Fig. S6A (ESI†) showed the nitrogen adsorption/desorption isotherms of Cur-MCM-41(1.7nm) and Cur-MCM-41(2.1nm) were typical type IV with clear capillary condensation steps in the relative pressure (P/P_0) range of 0.2-0.4. The details of surface area, pore volume, and pore size are given in Table S1, ESI†. After loading curcumin, the surface area and the pore volume decreased. However, the pore size remained the same (Fig. S6 B, ESI†). It is suggested that due to the hydrophobic nature of curcumin, the drug molecules tend to repel from the hydrophilic silanol groups on the surface and exist as isolated nano-aggregates inside the pore channels, thus the pore size after loading is not changed.

A hydrophilic drug (captopril) was also loaded into MCM-41 with a pore size of 2.1 nm by a wetting impregnation method. The N_2 sorption isotherm and pore size distribution

curve of MCM-41 after drug loading was shown in Fig. S7, ESI†. After drug loading the BET surface area decreased from 946 to 534 m^2/g, the pore volume from 0.66 to 0.38 cm^3/g, and pore size from 2.1 to 1.7 nm (Table S1, ESI†). These data suggest that the drug molecules were introduced into the mesopores. From the TGA analysis (Fig. S8, ESI†) it is confirmed that the weight percentage of captopril loaded is 16.4. Because captopril is hydrophilic in nature, the drug molecules may locate preferentially adjacent to the hydrophilic surface silanol, leading to a decrease pore size.

The drug loading is further confirmed by Fourier transform infrared (FTIR) studies (Fig S9, ESI†). FTIR spectra for the pure captopril showed peaks at 2880, 2955 and 2987 cm^{-1}, corresponding to asymmetrical C-H stretching vibration of captopril anion, and the characteristic bands at 2569, 1745, 1584 and 1475 cm^{-1} could be attributed to S-H, C=O of COOH group, C=O of amide and quaternary carbon atom respectively. A sharp peak at 3745 cm^{-1} can be observed for MCM-41, which is attributed to the isolated silanol groups and water molecules. The FT-IR spectrum of captopril loaded MCM-41 sample shows weak shoulder at 2959 cm^{-1} which is attributed to symmetrical CH_3 stretching mode of captopril and a band at 1749 cm^{-1} due to the COOH group on captopril.[30] The C=O of amide can be clearly observed at 1646 cm^{-1}, this shift is attributed to the weak interaction with the silanol groups on the surface of MCM-41. The signal from isolated silanol disappears for captopril loaded MCM-41. The corresponding peaks of the pure drug were observed in the Cap-MCM-41 particles, confirming that the drug was loaded effectively.

The *in-vitro* drug release profile of floating tablets was performed in SGF, pH 1.2 at 37 ºC using Rosette rise apparatus (RRA) to mimic the environment of stomach (Fig. S10, ESI†).[31] Four different formulations were studied to show the importance of MSNs and its pore size in the release profile of curcumin (Table S3, ESI†). The total weight of tablets for four formulations and the amount of curcumin in each tablet are the same. F1 and F4 are made with polymer and drug loaded MCM-41 with the pore size of 1.7 nm and 2.1 nm, respectively. F2 is the physical mixture of MCM-41 (2.1nm), polymer and drug. F3 is made of polymer and drug in the absence of MSNs. Fig. 2 showed the morphology of floating tablets (F1-F4) at different time points of dissolution study. The diffusion of dissolution medium into the tablets was clearly visible at 1 h as evidenced by the volume change. However, there was no disintegration of tablets suggesting effective binding ability of HPMC and MSNs.

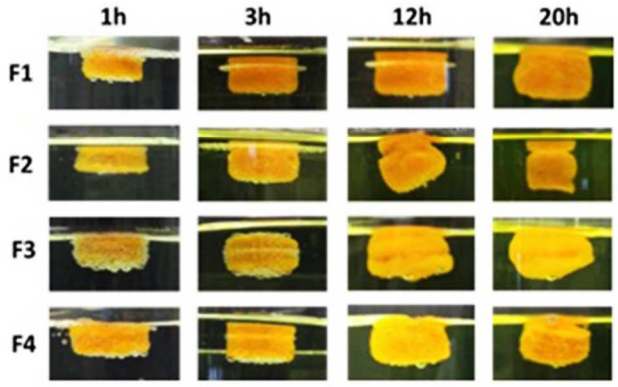

Fig. 2 The morphology of floating tablet at different time points. (F1) Cur-MCM-41(1.7nm), (F2) Physical mixture of curcumin and MCM-41, (F3) Pure curcumin, (F4) Cur-MCM-41(2.1nm). All the formulations contain polymer and sodium bicarbonate.

The release profiles of curcumin loaded floating tablet F1-F4 are shown in Fig. 3. The release rate of F4 Cur-MCM-41(2.1nm) was similar to conventional floating tablet F3. There is no significant difference in the release profile of F2 (floating tablet made from physical mixture) compared to F3 and F4. The dissolved curcumin from floating tablets was less than 19% at 20 h in three groups (F2-F4). Remarkably, the cumulative percentage drug release of F1 Cur-MCM-41(1.7nm) was twice that of conventional floating tablet at 20 h (42.8%). The solubility of a substance is a function of its particle size according to the Ostwald-Freundlich equation.[25] After loading curcumin into MSNs, the size of curcumin is dependent on the pore size of MSNs. The enhanced solubility of curcumin in F1 can be attributed to the use of MSNs with a carefully chosen pore size of 1.7 nm, which has been demonstrated before with the highest solubility enhancement. Additionally, it is noted that when curcumin was physically mixed with MSNs there was no improvement in release kinetics, indicating the encapsulation of curcumin into the nanopores is important for the solubility enhancement.

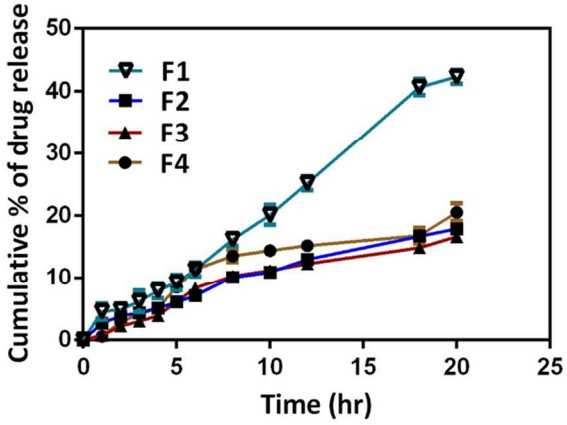

Fig. 3 The release profile of curcumin from floating tablets. (F1) Cur-MCM-41(1.7nm), (F2) Physical mixture of curcumin and MCM-41, (F3) Pure curcumin and (F4) Cur-MCM-41(2.1nm). All the formulations contain polymer and sodium bicarbonate.

For captopril floating tablets, two formulations were prepared. F5 was made from drug loaded MCM-41, while F6 using HPMC polymers in the absence of MCM-41 (Table S4, ESI†). As expected for F6 batch, 60% of captopril was released within the first 6 h, and almost 100% release was observed at 8 h (Fig. 4). This observation indicates that in the case of conventional polymer based floating tablets, swelling of HPMC

allows quick exposure of the drug molecules to dissolution medium, causing fast release of captopril into the SGF. While for floating tablet F5 made with MCM-41, a sustained drug release of captopril was observed reaching 100% only after 24 h. At all time points the release rate of floating tablet F5 was slower than that of conventional tablet F6. Because the drug molecules are pre-loaded inside the nanopores, the dissolution medium has to diffuse through two barriers: the polymer matrix to induce the gelation of HPMC and the nanopores in order to dissolve the drug molecules. Consequently, the floating tablet made from MSNs gives rise to more control over hydrophilic drugs.

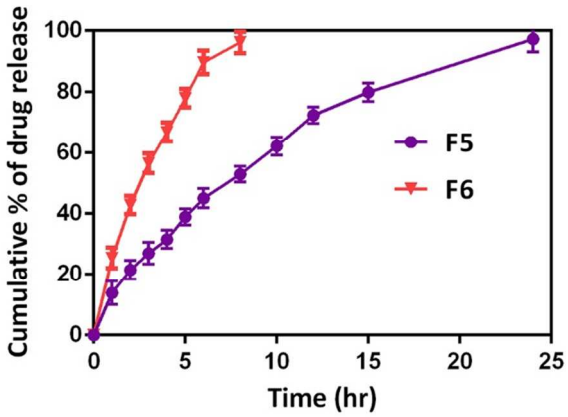

Fig. 4 The release profile of captopril from floating tablet. (F5) Cap- MCM-41, (F6) Pure captopril. All the formulations contain polymer and sodium bicarbonate.

In conclusion, we have successfully prepared a new generation of floating tablets using MSNs as a key formulation ingredient. With this finding, the advantages of mesoporous materials can be further integrated into floating tablets with fine control over the sustainable release of water-soluble drugs and, more importantly, enhancing the solubility of poorly water-soluble drugs, an issue that cannot be solved by conventional floating tablet technology. Our success has paved the way for formulation improvement in localised drug release.

We acknowledge the support from the Australian Research Council, the Queensland Government, the Australian National Fabrication Facility and the Australian Microscopy and Microanalysis Research Facility at the Centre for Microscopy and Microanalysis, The University of Queensland. We also thank The Pharmacy Australia Centre of Excellence for providing access to tablet punching machine.

Notes and references

[a] *Australian Institute of Bioengineering and Nanotechnology, The University of Queensland, Brisbane,QLD-4072, Australia. *Email: c.yu@uq.edu.au, a.popat@uq.edu.au Fax: +61-7-334 63973; Tel: +61-7-334 63283*
[b] *The School of Pharmacy, The University of Queensland, Brisbane, QLD 4072, Australia*
[c] *Mucosal Diseases Group, Mater Research Institute – The University of Queensland, Translational Research Institute, 37 Kent St, Woolloongabba, QLD 4102, Australia*

Electronic Supplementary Information (ESI) available: [details of any supplementary information available should be included here]. See DOI: 10.1039/c000000x/

1. C. T. Kresge, M. E. Leonowicz, W. J. Roth, J. C. Vartuli and J. S. Beck, *Nature*, 1992, **359**, 710-712.
2. V. Mamaeva, C. Sahlgren and M. Linden, *Adv Drug Deliv Rev*, 2013, **65**, 689-702.
3. D. Douroumis, I. Onyesom, M. Maniruzzaman and J. Mitchell, *Crit Rev Biotechnol*, 2013, **33**, 229-245.
4. C. Y. Lai, B. G. Trewyn, D. M. Jeftinija, K. Jeftinija, S. Xu, S. Jeftinija and V. S. Lin, *J Am Chem Soc*, 2003, **125**, 4451-4459.
5. K. K. Unger, D. Kumar, M. Grun, G. Buchel, S. Ludtke, T. Adam, K. Schumacher and S. Renker, *J Chromatogr A*, 2000, **892**, 47-55.
6. M. Grun, I. Lauer and K. K. Unger, *Adv Mater*, 1997, **9**, 254-&.
7. S. H. Wu, Y. Hung and C. Y. Mou, *Chem Commun*, 2011, **47**, 9972-9985.
8. X. Li, Q. R. Xie, J. X. Zhang, W. L. Xia and H. C. Gu, *Biomaterials*, 2011, **32**, 9546-9556.
9. Y. Gao, Y. Chen, X. F. Ji, X. Y. He, Q. Yin, Z. W. Zhang, J. L. Shi and Y. P. Li, *Acs Nano*, 2011, **5**, 9788-9798.
10. M. Liong, J. Lu, M. Kovochich, T. Xia, S. G. Ruehm, A. E. Nel, F. Tamanoi and J. I. Zink, *Acs Nano*, 2008, **2**, 889-896.
11. D. S. Lin, Q. Cheng, Q. Jiang, Y. Y. Huang, Z. Yang, S. C. Han, Y. N. Zhao, S. T. Guo, Z. C. Liang and A. J. Dong, *Nanoscale*, 2013, **5**, 4291-4301.
12. S. W. Song, K. Hidajat and S. Kawi, *Chem Commun*, 2007, 4396-4398.
13. K. Zhang, W. Wu, K. Guo, J. F. Chen and P. Y. Zhang, *Langmuir*, 2010, **26**, 7971-7980.
14. B. Tzankov, K. Yoncheva, M. Popova, A. Szegedi, G. Momekov, J. Mihaly and N. Lambov, *Micropor Mesopor Mat*, 2013, **171**, 131-138.
15. Y. P. Xu, F. Y. Qu, Y. Wang, H. M. Lin, X. A. Wu and Y. X. Jin, *Solid State Sci*, 2011, **13**, 641-646.
16. Y. Z. Zhang, J. C. Wang, X. Y. Bai, T. Y. Jiang, Q. Zhang and S. L. Wang, *Mol Pharmaceut*, 2012, **9**, 505-513.
17. V. D. Prajapati, G. K. Jani, T. A. Khutliwala and B. S. Zala, *J Control Release*, 2013, **168**, 151-165.
18. S. Strubing, H. Metz and K. Mader, *J Control Release*, 2008, **126**, 149-155.
19. G. P. Andrews, T. P. Laverty and D. S. Jones, *Eur J Pharm Biopharm*, 2009, **71**, 505-518.
20. V. A. Eberle, J. Schoelkopf, P. A. Gane, R. Alles, J. Huwyler and M. Puchkov, *Eur J Pharm Sci*, 2014, **58**, 34-43.
21. I. Jimenez-Martinez, T. Quirino-Barreda and L. Villafuerte-Robles, *Int J Pharm*, 2008, **362**, 37-43.
22. V. K. Pawar, S. Kansal, G. Garg, R. Awasthi, D. Singodia and G. T. Kulkarni, *Drug Deliv*, 2011, **18**, 97-110.
23. B. N. Singh and K. H. Kim, *J Control Release*, 2000, **63**, 235-259.
24. A. O. Nur and J. S. Zhang, *Int J Pharm*, 2000, **194**, 139-146.
25. S. Jarnbhrunkar, M. H. Yu, J. Yang, J. Zhang, A. Shrotri, L. Endo-Munoz, J. Moreau, G. Q. Lu and C. Z. Yu, *J Am Chem Soc*, 2013, **135**, 8444-8447.
26. Y. Zhang, Z. Zhi, T. Jiang, J. Zhang, Z. Wang and S. Wang, *J Control Release*, 2010, **145**, 257-263.
27. S. Yang, L. Z. Zhao, C. Z. Yu, X. F. Zhou, J. W. Tang, P. Yuan, D. Y. Chen and D. Y. Zhao, *J Am Chem Soc*, 2006, **128**, 10460-10466.
28. L. Mercier and T. J. Pinnavaia, *Environ Sci Technol*, 1998, **32**, 2749-2754.
29. J. S. Beck, J. C. Vartuli, W. J. Roth, M. E. Leonowicz, C. T. Kresge, K. D. Schmitt, C. T. W. Chu, D. H. Olson, E. W. Sheppard, S. B. Mccullen, J. B. Higgins and J. L. Schlenker, *J Am Chem Soc*, 1992, **114**, 10834-10843.
30. I. F. Alexa, M. Ignat, R. F. Popovici, D. Timpu and E. Popovici, *Int J Pharm*, 2012, **436**, 111-119.
31. P. Arya and K. Pathak, *Int J Pharm*, 2014, **460**, 1-12.

Graphical Abstract

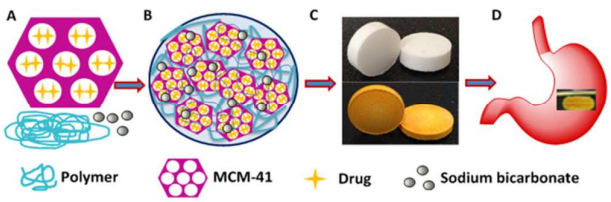

Floating tablets were made with hydrophobic (curcumin) and hydrophilic (captopril) drug loaded mesoporous silica nanoparticles respectively, leading to improved dissolution rate of curcumin and controlled release for captopril.